Accepted Manuscript

Short Communication

High Specific Strength And Stiffness Structures Produced Using Selective Laser Melting

Vivien J. Challis, Xiaoxue Xu, Lai Chang Zhang, Anthony P. Roberts, Joseph F. Grotowski, Timothy B. Sercombe

PII: S0261-3069(14)00441-5
DOI: http://dx.doi.org/10.1016/j.matdes.2014.05.064
Reference: JMAD 6542

To appear in: *Materials and Design*

Received Date: 8 April 2014
Accepted Date: 28 May 2014

Please cite this article as: Challis, V.J., Xu, X., Zhang, L.C., Roberts, A.P., Grotowski, J.F., Sercombe, T.B., High Specific Strength And Stiffness Structures Produced Using Selective Laser Melting, *Materials and Design* (2014), doi: http://dx.doi.org/10.1016/j.matdes.2014.05.064

HIGH SPECIFIC STRENGTH AND STIFFNESS STRUCTURES PRODUCED USING SELECTIVE LASER MELTING

Vivien J. Challis[1,*], Xiaoxue Xu[2,†], Lai Chang Zhang[3], Anthony P. Roberts[1], Joseph F. Grotowski[1], Timothy B. Sercombe[2]

1. School of Mathematics and Physics, The University of Queensland, St Lucia, QLD 4072, Australia
2. School of Mechanical and Chemical Engineering, The University of Western Australia, Perth, WA 6009, Australia
3. School of Engineering, Edith Cowan University, Perth, WA 6027, Australia
* Corresponding author. Phone: +61 7 336 52302. Email: vchallis@maths.uq.edu.au

Abstract

Selective Laser Melting (SLM) was used to fabricate scaffolds using the titanium alloy Ti-6Al-4V. Two types of high porosity open-cell structures were manufactured: the first built from topology optimised designs with maximised stiffness, and the second from gyroid labyrinths. In mechanical compression tests the scaffolds demonstrate exceptional strength- and stiffness-to-weight ratios. In particular, for densities in the range 0.2 – 0.8 g/cm^3 the topology optimised scaffolds have specific strength and stiffness that are superior to those of comparable materials in the literature. In addition, the optimised scaffolds have the benefit of being elastically isotropic. The results of finite element calculations accurately match the measured stiffness of the scaffolds. Calculated strain energy distributions provide insight into how the high stiffness and strength of the optimised designs is connected to their efficient distribution of load.

Keywords: Selective laser melting; strength; Young's modulus; titanium; finite element analysis

1. Introduction

Light-weight porous materials are becoming increasingly attractive for a number of applications. They are used to reduce weight in automotive and aerospace industries, improve thermal insulation properties, increase noise and vibration suppression and match bone stiffness and aid osseointegration of medical implants [1]. In addition, they are used as a core in composite sandwich construction and in a variety of filter applications. There are a number of different methods for the production of porous materials (see, e.g., [2]). Examples include the foaming of liquid metals, conventional press-and-sinter powder metallurgy using space holders, replication, and additive manufacturing (AM) techniques such as Selective Laser

† Present address: Department of Chemistry and Biomolecular Sciences, Macquarie University, Sydney, NSW 2109, Australia

Melting (SLM). Among these methods, only AM offers the opportunity to produce complex three-dimensional purpose-designed structures.

Additive manufacturing covers a group of advanced manufacturing technologies that fabricate parts directly from a computer solid model without the need for an expensive tool or die set. These techniques are unrivalled in their ability to produce parts with almost no geometrical constraints. One such AM technique is SLM, whereby metal powder is melted using a high intensity infrared laser beam that traces the geometry of each layer. After exposure of a layer, the build chamber descends ~50 μm, a fresh layer of powder is spread on top and the next layer is produced. This process continues until the part is complete. Due to its layer-by-layer nature, AM facilitates the fabrication of porous open cell scaffolds with complex internal architectures by allowing precise control of the porosity (including pore size, shape and interconnectivity). As SLM requires the removal of unmelted powder from within the structure, it is not possible to use SLM to create closed-cell "foams". The requirement to maintain open porosity is an advantage for applications such as bone replacements or filtration, although the requirement to maintain open porosity does result in a decrease in the theoretically attainable strength and stiffness [3]. This paper presents an analysis of open-cell materials produced with AM and shows that they have exceptionally high stiffness and strength.

Given its high strength and stiffness to weight ratios, titanium is a natural choice for producing parts with SLM. Its applications include light-weight and energy absorbing structures [4, 5], biomedical scaffolds [6-14], and cores for sandwich construction [15-17]. To date, the emphasis has been on structures produced from relatively simple unit cells, including BCC/octahedral [4, 5, 12, 15, 17], rhombic dodecahedron [13], tetrahedral [6] and auxetic [18] structures. The flexibility of the SLM manufacturing process means that it is possible to design a structure for function, rather than to satisfy the geometric constraints of the manufacturing process. Unit cells that are particularly optimised for high specific strength and stiffness could significantly improve the overall properties of these structures. The resultant constrained optimisation problem is suited to the framework of topology optimisation (see, e.g., [19]), which does not *a priori* prescribe the geometry or connectivity of the structure.

Two types of open cell, periodic scaffold architectures are considered in this paper. The "gyroid" (Figure 1(a)) structure has previously been proposed as being particularly suited to additive manufacturing as it is self-supporting and can be built over a wide range of cell sizes with good agreement to the original CAD models [20, 21]. The "optimised" (Figure 1(b)) structure has been specifically designed using topology optimisation to have high stiffness. It is natural to expect that this structure will have high strength, but it is important to verify this experimentally.

2. Methods

Approximate gyroid labyrinths were generated using an implicit surface representation via the function

$$f(x,y,z) = \alpha - (\sin y \cos x + \sin x \cos z + \sin z \cos y), \quad (1)$$

where α is chosen to give the desired solid fraction, and x, y and z are the three spatial directions that each range over an interval of length 2π to generate a single unit cell. Values of $f(x,y,z)$ less than zero specify points inside the solid scaffold. This approximate representation arises from the simplest Fourier component expansion of the gyroid minimal surface (e.g., [22]). Gyroid scaffolds were generated at nominal solid fractions of approximately 5%, 10% and 15% using α values of 1.32, 1.125 and 1.06, respectively. The "optimised" unit cells at solid fractions between 7% and 20% were generated using the level set method of topology optimisation, as documented in previous work [23, 24]. The objectives in the optimisation problem were a linear combination of the bulk modulus of the scaffold and the diffusivity within the pore space. In addition, the scaffolds were required to be macroscopically isotropic. This is a proxy for optimising the Young's modulus for every loading direction. Optimised scaffolds at a higher solid fraction as found previously [23] were used as starting structures for the optimisation. However, a higher computational resolution of $60 \times 60 \times 60$ elements within the base cell was required to facilitate the generation of optimised scaffolds at solid fractions below 20%. The scaffold representations were smoothed prior to manufacture via SLM.

Scaffolds were manufactured on a Realizer SLM100 machine using Ti-6Al-4V powder sourced from TLS Technik in Germany. The details of the powder are shown below in Table 1, while the processing parameters are summarised in Table 2. The following scanning strategy was used: each layer was divided into areas that had at least one layer of solid below ("on solid") and those that were built "on powder" (the overhangs/downward facing surfaces). Due to the lower thermal conductivity of powder compared to solid, the "on powder" areas require a lower laser energy, which was achieved through the use of a lower laser power. Layers were scanned using a contour and fill approach, and the direction of the fill vectors were rotated 90° from one layer to the next. The layer thickness, laser scan spacing and beam compensation were kept constant at 0.05mm, 0.1mm and 0.15mm, respectively.

Figure 2 shows stereo microscope photographs of the fabricated SLM scaffolds at a nominal solid fraction of 10%. After fabrication, the scaffolds were separated from the substrate and the support structure was removed. The scaffolds were then glass-bead blasted to remove any lightly bonded powder and finally cleaned with compressed air. The dimensions and weight were measured to a precision of 0.01mm and 0.001g, respectively, in order to determine the overall density of the structure.

Initially, scaffolds containing 5 x 5 x 10 unit cells were tested in compression on an Instron 5982. The strain in the sample was determined by averaging the reading from two 10 mm extensometers on opposite sides of the sample. Unit cell sizes of 3.33mm and 5 mm were used, meaning that the 10mm extensometers located correctly on the flat sections of the

samples. The scaffolds were cycled five times at 0.5mm/min to approximately 50% of the yield point. The Young's modulus was calculated on the last four of these cycles and averaged to give a single data point. After the last cycle, the load was increased at the same strain rate until failure occurred.

To increase the number of strength measurements and test for boundary effects, additional samples of cell size 3.33 mm in configurations of 3 x 3 x 3, 5 x 5 x 5 and 7 x 7 x 7 cells were compressed at a cross-head speed of 0.5mm/min until failure. The results showed little variation in strength with different numbers of unit cells. Most of these additional samples were too small for Young's modulus testing using 10 mm extensometers.

The mechanical properties of the bulk material fabricated by SLM were determined according to ASTM: E8 on samples aligned to the x-axis of the SLM machine. The average and standard deviation of the yield strength, tensile strength and strain to failure of 5 samples was 1075 ± 20 MPa, 1160 ± 8 MPa and 2.5 ± 0.3%, respectively. Young's Modulus was determined using an IMCE Resonant Frequency & Damping Analyser to be 109 ± 3 GPa.

3. Results and Discussion

Figure 3 shows the modulus as a function of bulk density for the gyroid and optimised structures alongside data reported in the literature for comparable-density titanium foams, and Selective Laser and Electron Beam Melted (EBM) titanium. The stiffness of the scaffolds was also calculated via a finite element analysis (FEA) utilising hexahedral finite elements. Pixel-based representations of the gyroid scaffolds using 60 × 60 × 60 pixels were generated from the implicit surface representation for this purpose. Details of the analysis technique have been reported previously [23]. The experimentally determined modulus for both scaffold types is in excellent agreement with the predicted stiffness calculated from finite element analysis (Figure 3). This is consistent with previous work using other materials [23].

The Young's modulus of the optimised structures is greater than that of the gyroid and all modulus values obtained from the literature, with the exception of the SLM-produced titanium "cubic-lattice" scaffolds by Sallica-Leva et al. [25]. These structures can be visualised as a periodic array of interconnected three-dimensional crosses, or as a stack of joined cubes with solid edges (the faces and centre forming a pore). An important difference between this cubic-lattice structure and the optimised structure is that the former is highly anisotropic. It has axis-aligned straight members that traverse the sample so it is stiff (and strong) when loaded along these axes [25] but would be expected to be significantly more compliant if loaded diagonally. To verify this, a finite element calculation was performed on the same cubic lattice structure at 80% porosity. The Young's modulus for the cubic lattice structure varies significantly with direction as shown in Figure 4(a). Specifically, this structure would have only 16% of the axis-aligned modulus when loaded along a diagonal direction ([1,1,1]) (c.f., Ref. [23] for further discussion). In contrast, the optimised structures are designed to be isotropic. At 80% porosity, the Young's modulus variation is as depicted

in Figure 4(b), and is the same for all directions to within less than 1%. This is a significant benefit of the optimised structure if a scaffold is required to support off-axis loads.

Figure 5 shows the strength of the gyroid and optimised structures as a function of density. Similar to Figure 3, Figure 5 shows that the optimised structure is superior to the gyroid and also to the other data in the literature. As for the stiffness, the cubic-lattice SLM structures [25] have high strength when loaded along their struts, but as discussed above for stiffness, their strength may be significantly lower if loaded diagonally. It is apparent that the optimised scaffolds have excellent specific stiffness and specific strength and also have the advantage of being elastically isotropic.

In order to understand why the optimised structure is superior to the gyroid, it is instructive to examine the computed element by element distribution of strain energy density within each unit cell under a vertical uniaxial compression. The energy density gives a simple scalar representation of the stress and deformation at each point in the structure. Histograms for the gyroid and optimised structures at a 10% nominal solid fraction are shown in Figure 6(a) and (b). It is clear that the gyroid has elements with much higher strain energy density than those within the optimised structure. The implied high deformation within the gyroid structure reflects its lower Young's modulus. Importantly, the histogram Figure 6(b) illustrates that the optimised structure is far more efficient at distributing load throughout the structural elements; fewer elements are highly stressed, while many more elements carry comparatively moderate stresses. Again, this is connected to the relatively high modulus of the optimised structure.

Selective Laser Melted components are not fully dense and the inherent porosity is likely to result in the material having a higher strength in compression than tension. This will be particularly true when the material has low ductility. Due to the rapid cooling experienced by the material during Selective Laser Melting, as processed Ti-6Al-4V tends to form low ductility martensitic α' structures [9, 25-27]. As such, the strain to failure of the bulk material is low (2.5 ± 0.3%). To study the distribution of tension and compression within the scaffolds, the strain energies in Figure 6(a) and (b) are separated into compressive and tensile strain energies. At each point in the scaffold, the sign of the strain energy density is chosen to match the sign of the first principal stress and has been plotted in Figure 6(c) and (d). The tensile elements occur in lateral struts that are stretched as the scaffold is vertically compressed, as seen in visualisations of the FEA data that are shown in Figure 7. Given the low ductility nature of the SLM material, it is likely that the struts under the highest tensile loading will fail first. This has recently been verified through the use of in situ micro CT [28]. It is apparent from Figure 6(c) and (d) as well as from Figure 7 that the optimised structure contains significantly lower levels of tensile strain energies than the gyroid. The obvious interpretation is that the more efficient load distribution within the optimised structure is responsible for its greater strength.

4. Conclusions

This paper has shown that structures designed using topology optimisation have exceptional strength and stiffness to weight ratios. These optimised and gyroid structures were produced in Ti-6Al-4V using Selective Laser Melting, an additive manufacturing technique which is ideal for producing high complexity metallic parts. Finite element calculations accurately predict the stiffness of two very different geometries over a range of solid fractions. The finite element analysis reveals the efficiency of the optimised structure, giving insight into its high specific strength. This work could be expanded to a range of different unit cells. This will point towards methods of designing stronger, light-weight porous materials and facilitate the development of a theory of the strength of porous, open cell materials.

Acknowledgements: This research was supported under the Australian Research Council's Discovery Projects funding scheme (project number DP110101653) and a UWA-UQ Bilateral Research Collaboration Award.

References

[1] Ashby MF, Evans AG, Fleck NA, Gibson LJ, Hutchinson JW, Wadley HNG. Metal Foams: A Design Guide. Woburn, MA: Butterworth-Heinemann; 2000.
[2] R. Singh, P. D. Lee, Dashwood RJ, Lindley TC. Titanium foams for biomedical applications: a review. Materials Technology. 2010;25:127-36.
[3] Gibson LJ, Ashby MF. Cellular Solids: Structure and Properties, 2nd Edition: Cambridge University Press; 1999.
[4] Gorny B, Niendorf T, Lackmann J, Thoene M, Troester T, Maier HJ. In situ characterization of the deformation and failure behavior of non-stochastic porous structures processed by selective laser melting. Materials Science and Engineering: A. 2011;528:7962-7.
[5] Smith M, Guan Z, Cantwell WJ. Finite Element Modelling of the Compressive Response of Lattice Structures Manufactured Using the Selective Laser Melting Technique. International Journal of Mechanical Sciences.
[6] Heinl P, Körner C, Singer RF. Selective Electron Beam Melting of Cellular Titanium: Mechanical Properties. Advanced Engineering Materials. 2008;10:882-8.
[7] Fukuda A, Takemoto M, Saito T, Fujibayashi S, Neo M, Pattanayak DK, et al. Osteoinduction of porous Ti implants with a channel structure fabricated by selective laser melting. Acta Biomaterialia. 2011;7:2327-36.
[8] Pattanayak DK, Fukuda A, Matsushita T, Takemoto M, Fujibayashi S, Sasaki K, et al. Bioactive Ti metal analogous to human cancellous bone: Fabrication by selective laser melting and chemical treatments. Acta Biomaterialia. 2011;7:1398-406.
[9] Murr LE, Quinones SA, Gaytan SM, Lopez MI, Rodela A, Martinez EY, et al. Microstructure and mechanical behavior of Ti–6Al–4V produced by rapid-layer manufacturing, for biomedical applications. Journal of the Mechanical Behavior of Biomedical Materials. 2009;2:20-32.
[10] Wang Y, Shen Y, Wang Z, Yang J, Liu N, Huang W. Development of highly porous titanium scaffolds by selective laser melting. Materials Letters. 2010;64:674-6.
[11] Mullen L, Stamp RC, Brooks WK, Jones E, Sutcliffe CJ. Selective Laser Melting: A regular unit cell approach for the manufacture of porous, titanium, bone in-growth constructs, suitable for orthopedic applications. Journal of Biomedical Materials Research Part B: Applied Biomaterials. 2009;89B:325-34.
[12] Sun J, Yang Y, Wang D. Mechanical properties of a Ti6Al4V porous structure produced by selective laser melting. Materials & Design. 2013;49:545-52.
[13] Campoli G, Borleffs MS, Amin Yavari S, Wauthle R, Weinans H, Zadpoor AA. Mechanical properties of open-cell metallic biomaterials manufactured using additive manufacturing. Materials & Design. 2013;49:957-65.
[14] Hsu H-C, Wu S-C, Hsu S-K, Tsai M-S, Chang T-Y, Ho W-F. Processing and mechanical properties of porous Ti–7.5Mo alloy. Materials & Design. 2013;47:21-6.
[15] Hasan R, Mines R, Fox P. Characterization of selectively laser melted Ti-6Al-4;V micro-lattice struts. Procedia Engineering. 2011;10:536-41.
[16] Mines RAW. On the characterisation of foam and micro-lattice materials used in sandwich construction. Strain. 2008;44:71-83.
[17] Hasan R, Mines R, Shen E, Tsopanos S, Cantwell W, Brooks W, et al. Comparison of the drop weight impact performance of sandwich panels with aluminium honeycomb and titanium alloy micro lattice cores. Applied Mechanics and Materials. 2010;24-25:413-8.

[18] Yang L, Harrysson O, West H, Cormier D. Compressive properties of Ti–6Al–4V auxetic mesh structures made by electron beam melting. Acta Materialia. 2012;60:3370-9.
[19] Bendsøe MP, Sigmund O. Topology optimization : theory, methods, and applications. Berlin ; New York: Springer; 2003.
[20] Yan C, Hao L, Hussein A, Raymont D. Evaluations of cellular lattice structures manufactured using selective laser melting. International Journal of Machine Tools and Manufacture. 2012;62:32-8.
[21] Hao L, Raymont D, Yan C, Hussein A, Young P. Design and additive manufacturing of cellular lattice structures. Innovative Developments in Virtual and Physical Prototyping: CRC Press; 2011. p. 249-54.
[22] CA Lambert, Radzilowski L, Thomas E. Curved Surfaces in Chemical Structure. Philosophical Transactions: Mathematical, Physical and Engineering Sciences 1996;354:2009-23.
[23] Challis VJ, Roberts AP, Grotowski JF, Zhang L-C, Sercombe TB. Prototypes for Bone Implant Scaffolds Designed via Topology Optimization and Manufactured by Solid Freeform Fabrication. Advanced Engineering Materials. 2010;12:1106-10.
[24] Challis VJ, Roberts AP, Wilkins AH. Design of three dimensional isotropic microstructures for maximized stiffness and conductivity. International Journal of Solids and Structures. 2008;45:4130-46.
[25] Sallica-Leva E, Jardini AL, Fogagnolo JB. Microstructure and mechanical behavior of porous Ti–6Al–4V parts obtained by selective laser melting. Journal of the Mechanical Behavior of Biomedical Materials. 2013;26:98-108.
[26] Thijs L, Verhaeghe F, Craeghs T, Humbeeck JV, Kruth J-P. A study of the microstructural evolution during selective laser melting of Ti–6Al–4V. Acta Materialia. 2010;58:3303-12.
[27] Luca Facchini, Emanuele Magalini, Pierfrancesco Robotti, Alberto Molinari, Simon Höges, Wissenbach K. Ductility of a Ti-6Al-4V alloy produced by selective laser melting of prealloyed powders. Rapid Prototyping Journal. 2010;16:450-45.
[28] Sercombe TB. Failure modes in high strength and stiffness to weight scaffolds produced by Selective Laser Melting, . submitted to Acta Materialia Feb 2014. .
[29] Cheng XY, Li SJ, Murr LE, Zhang ZB, Hao YL, Yang R, et al. Compression deformation behavior of Ti–6Al–4V alloy with cellular structures fabricated by electron beam melting. Journal of the Mechanical Behavior of Biomedical Materials. 2012;16:153-62.
[30] Heinl P, Müller L, Körner C, Singer RF, Müller FA. Cellular Ti–6Al–4V structures with interconnected macro porosity for bone implants fabricated by selective electron beam melting. Acta Biomaterialia. 2008;4:1536-44.
[31] Singh R, Lee PD, Jones JR, Poologasundarampillai G, Post T, Lindley TC, et al. Hierarchically structured titanium foams for tissue scaffold applications. Acta Biomaterialia. 2010;6:4596-604.
[32] Singh R, Lee PD, Lindley TC, Kohlhauser C, Hellmich C, Bram M, et al. Characterization of the deformation behavior of intermediate porosity interconnected Ti foams using micro-computed tomography and direct finite element modeling. Acta Biomaterialia. 2010;6:2342-51.
[33] Wen CE, Mabuchi M, Yamada Y, Shimojima K, Chino Y, Asahina T. Processing of biocompatible porous Ti and Mg. Scripta Materialia. 2001;45:1147-53.

Figure captions:

Figure 1: Visualizations of 2 × 2 × 2 base cells of the (a) gyroid and (b) optimised scaffolds at a 10% nominal solid fraction.

Figure 2. Stereo microscope photographs of manufactured (a) gyroid and (b) optimised scaffolds at a 10% nominal solid fraction.

Figure 3. Modulus as a function of density for the gyroid and optimised scaffold structures. Also shown is the prediction from FEA, the Ashby-Gibson model for open porous foams [3], and data from the literature [18, 20, 25, 29-33].

Figure 4. Young's modulus as calculated from FEA for (a) the cubic lattice structure from Sallica-Leva et al. [22] and (b) the topology optimised structure, both at 80% porosity. At any point on the surface, the distance to the origin indicates the Young's modulus when the scaffold is loaded along the direction toward the origin. The two surfaces (a) and (b) share the same scale.

Figure 5. Strength of the gyroid and optimised structures as a function of density. Also shown is data from the literature [11, 18, 20, 25, 29-33].

Figure 6. The strain energy density distribution within the gyroid (a, c) and optimised (b, d) structure at a 10% nominal solid fraction under a vertical compression load of 10 MPa. The vertical axis shows the proportion of solid elements. The base material is prescribed a Young's modulus of 100 GPa and a Poisson's ratio of 0.3. In (c) and (d), the sign of the strain energy density is determined by the sign of the first principal stress (positive corresponds to tension and negative to compression). The vertical arrows indicate the maximum and, in the case of (c) and (d), minimum values of the strain energy density.

Figure 7. Visualisations of the signed strain energy density within the (a) gyroid and (b) optimised structure at a 10% nominal solid fraction. The loading and material properties are the same as in Figure 6. Note the different scales on the colour bars for (a) and (b).

Tables:

Table 1. Selected characteristics of the Ti-6Al-4V powder (TLS Technik GmbH) used in this work.

Powder Composition (wt%)						**Powder Size (μm)**		
Ti	**Al**	**V**	**O**	**N**	**Fe**	**d_{10}**	**d_{50}**	**d_{90}**
Balance	6.25	4.04	0.14	0.02	0.22	25	37	51

Table 2. Laser parameters used.

	On Powder Setting		**On Solid Setting**	
Parameter	**Contour**	**Fill**	**Contour**	**Fill**
Laser Power (W)	100	140	140	200
Scan Speed (mm/s)	1500	1500	1500	1250

Figure 1

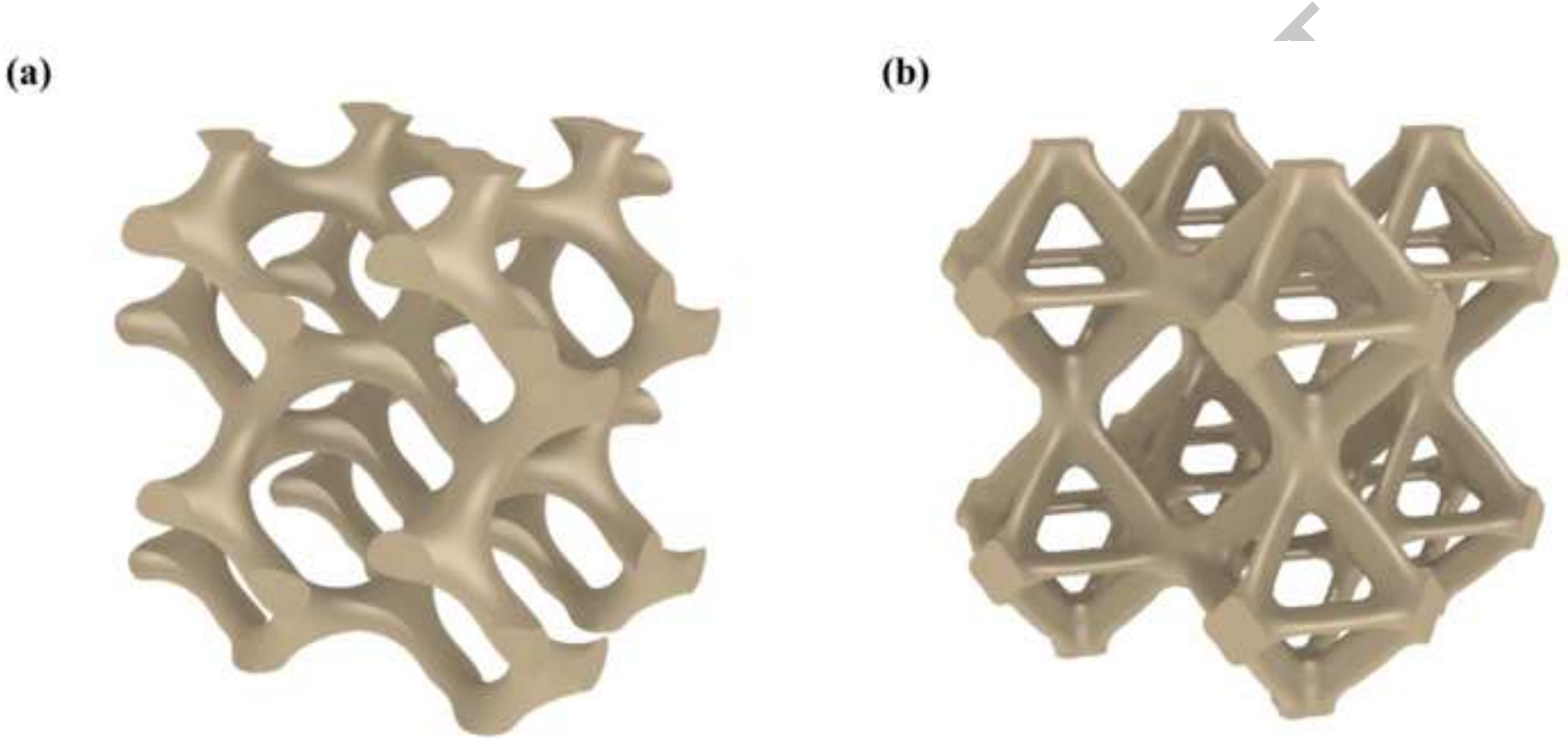

Figure 2

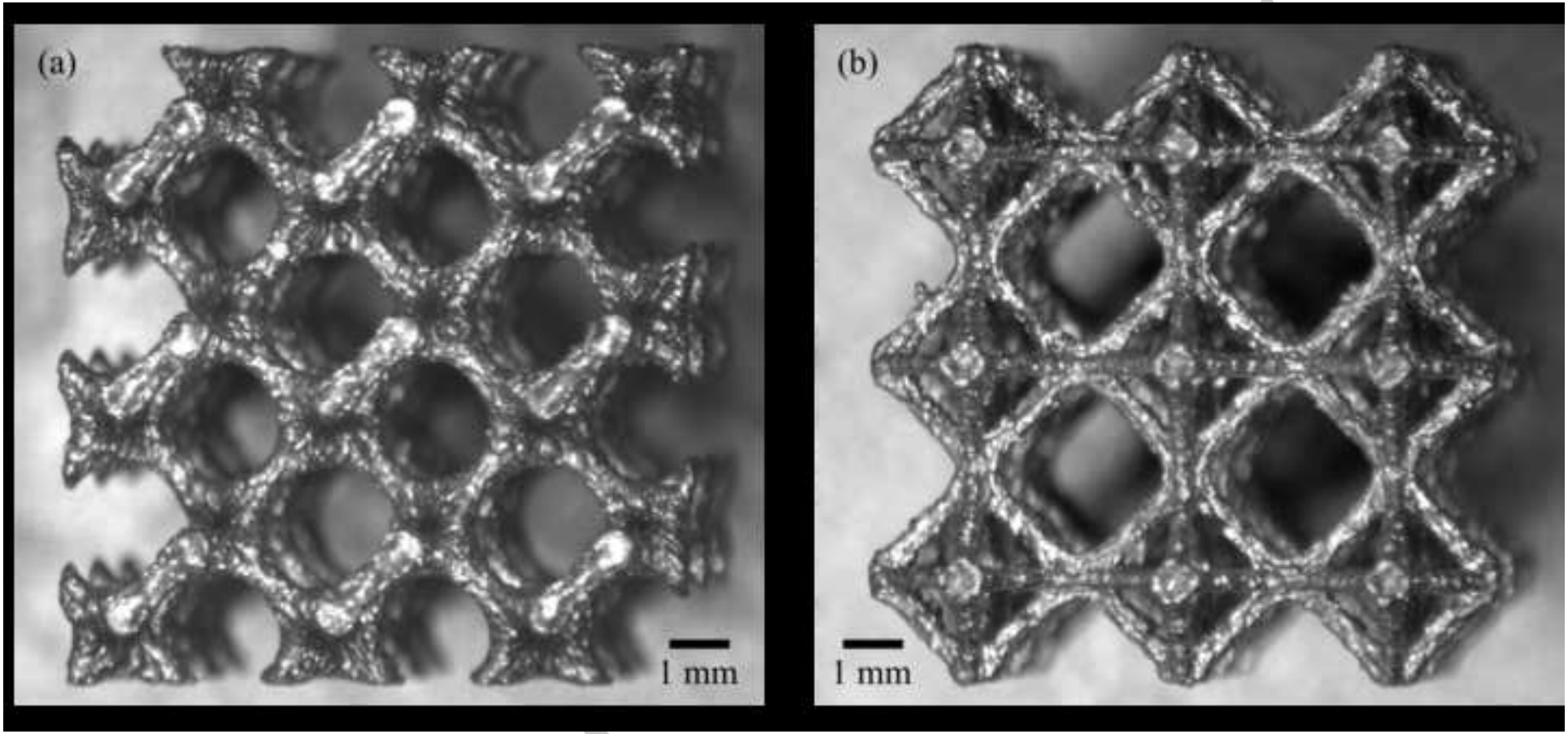

Figure 3

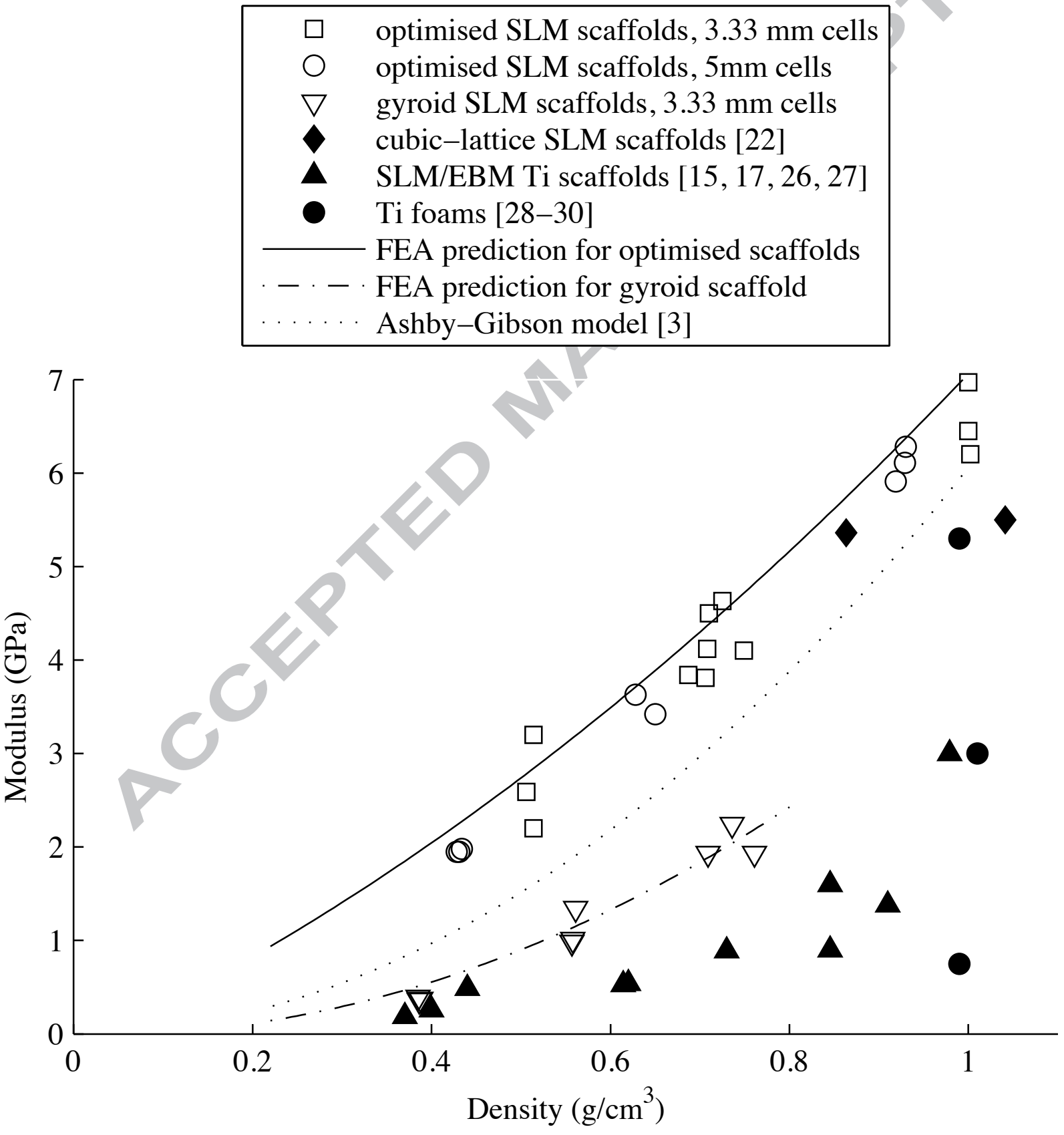

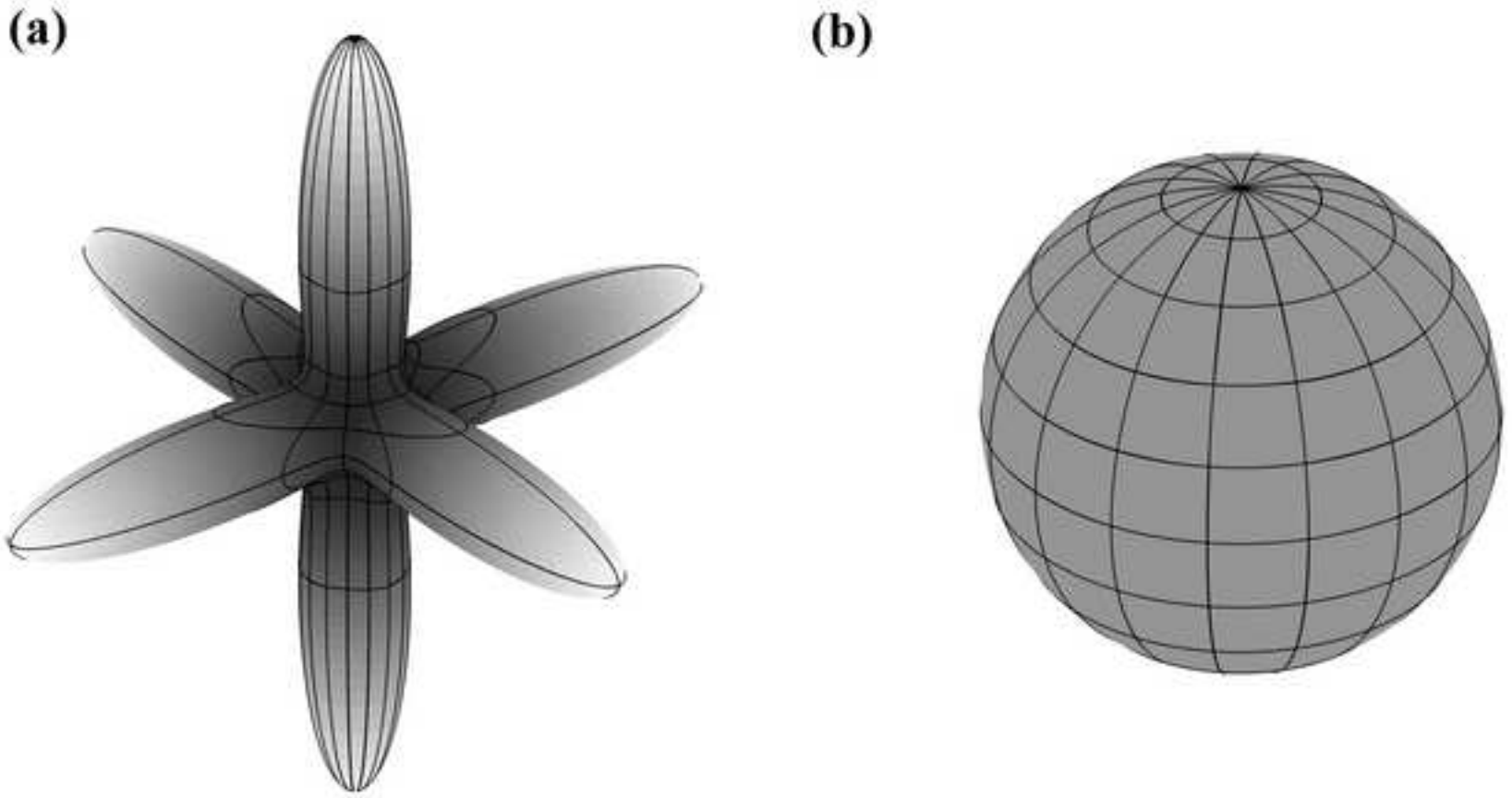

Figure 5

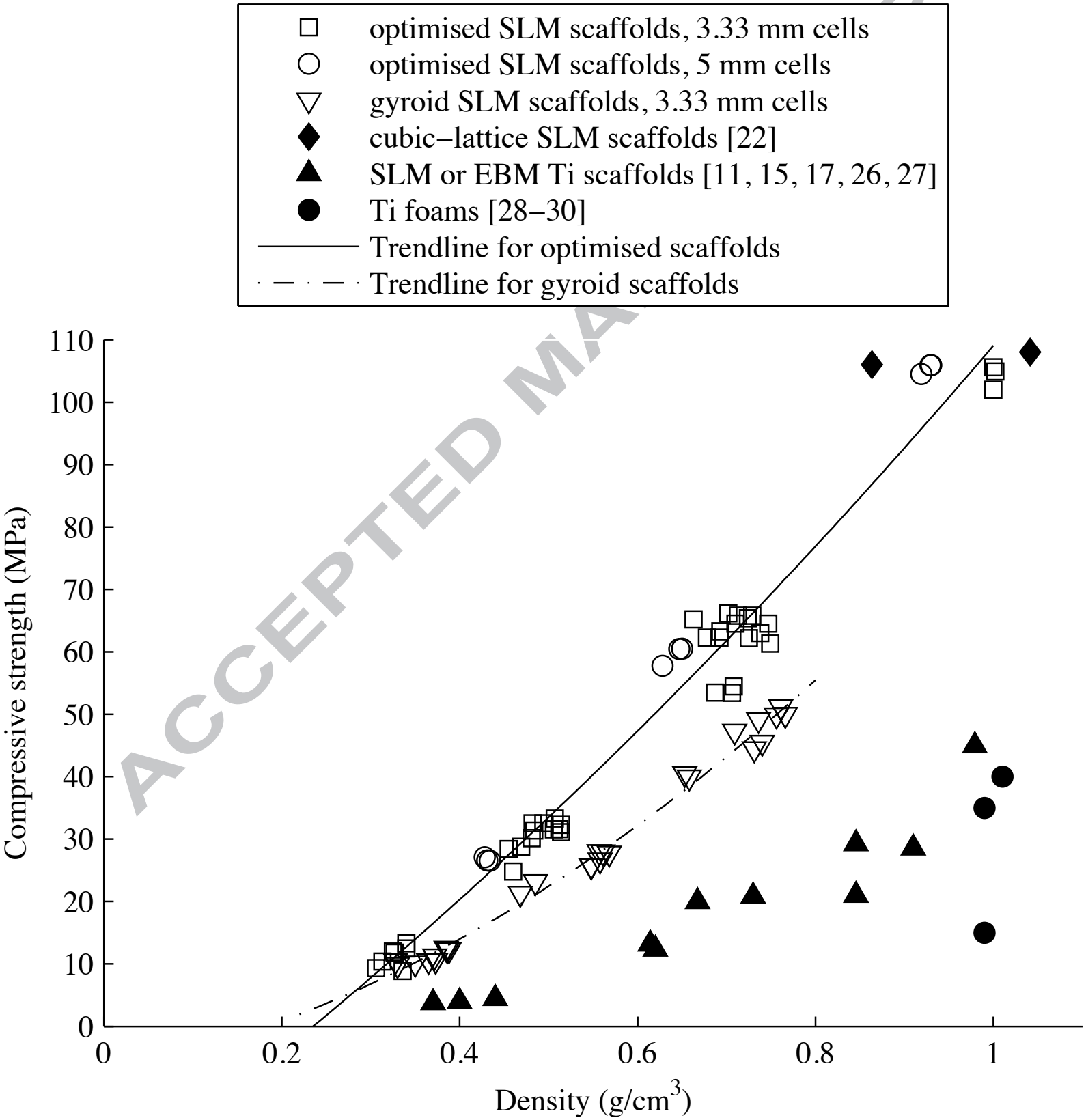

Figure 6

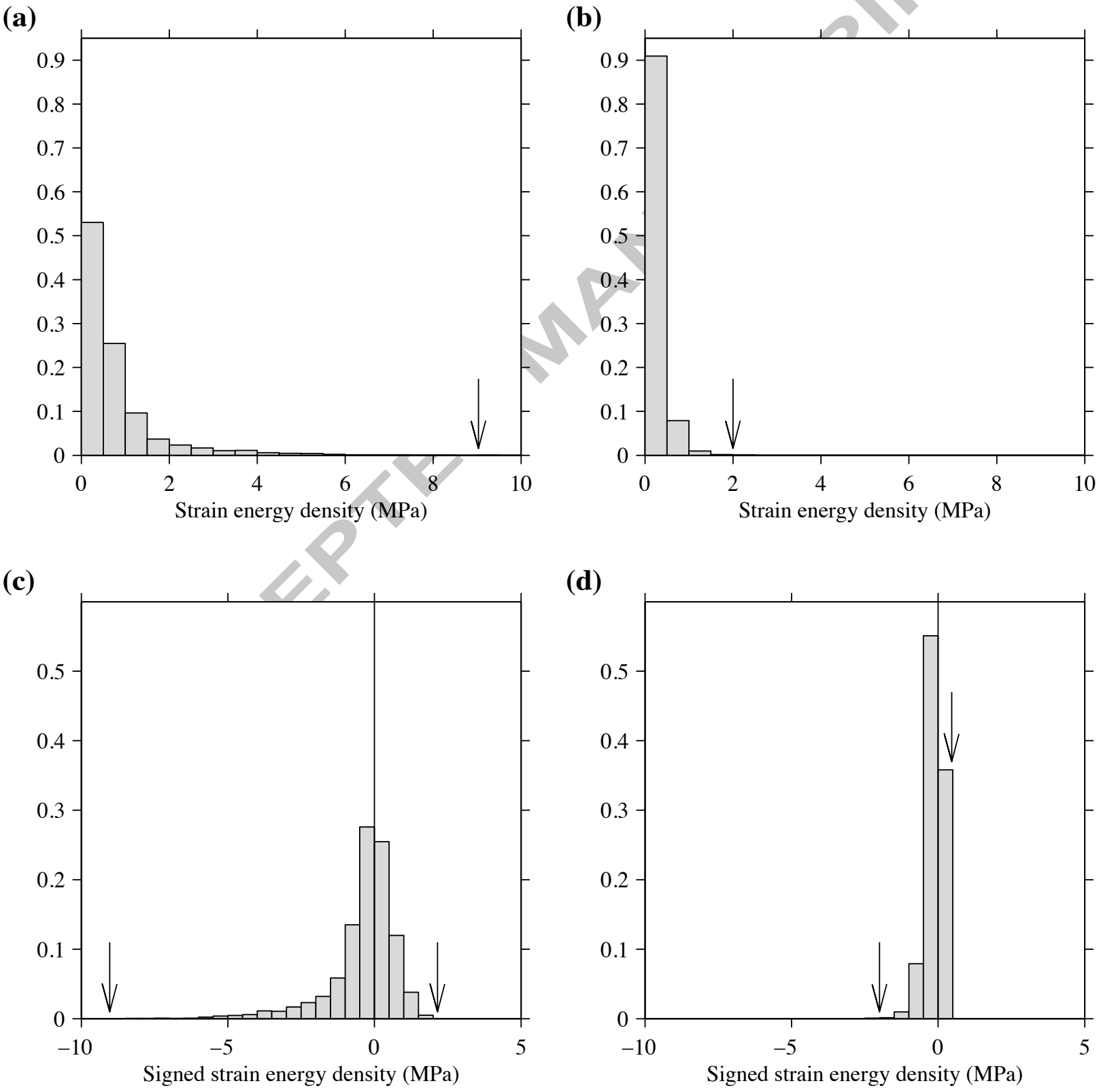

Figure 7

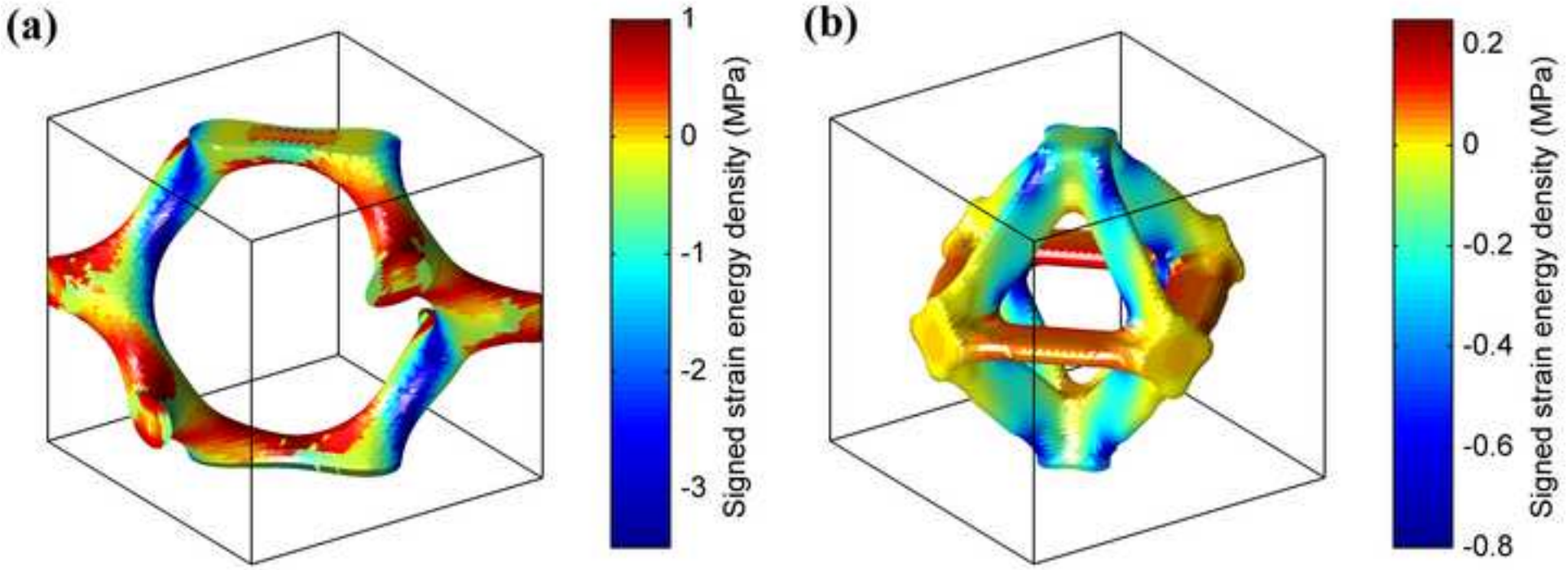

Highlights:

- Open-cell gyroid labyrinths and topology optimised structures are considered.
- Selective Laser Melting (SLM) is used for fabrication with titanium (Ti-6Al-4V).
- Topology optimised SLM scaffolds have exceptional specific strength and stiffness.
- Finite element analysis reveals the efficiency of the optimised structure.